Epitaxially grown $Fe_{16}N_2$ single-crystal films with high saturation magnetization prepared by facing targets sputtering

1995 J. Phys.: Condens. Matter 7 3667

(http://iopscience.iop.org/0953-8984/7/18/028)

J. Phys.: Condens. Matter 7 (1995) 3667–3674. Printed in the UK

Epitaxially grown $Fe_{16}N_2$ single-crystal films with high saturation magnetization prepared by facing targets sputtering

D C Sun†‡, C Lin§ and E Y Jiang§

† Department of Applied Physics, Tianjin University, Tianjin 300072, People's Republic of China

‡ Department of Materials Science and Engineering, Tsinghua University, Beijing 100084, People's Republic of China

§ Department of Applied Physics, Tianjin University, Tianjin 300072, People's Republic of China

Received 12 December 1994

Abstract. α''-$Fe_{16}N_2$ single-crystal films were prepared with a facing targets sputtering (FTS) system onto single-crystal NaCl substrates, at a deposition rate as high as 2.0 Å s^{-1}. In the process of deposition, the partial pressures of argon and nitrogen gases were held at 0.3 Pa and 0.05 Pa, respectively. The effect of the substrate temperature on the formation of Fe–N phases was investigated in detail. The crystal structure of the Fe–N films was examined with an x-ray diffractometer and a transmission electron microscope. At $T_s = 150\,°C$, single-crystal α''-$Fe_{16}N_2$ grows epitaxially on α-Fe with an orientation relationship of α''-$Fe_{16}N_2$ (110)//α-Fe (110), $Fe_{16}N_2$ [$\bar{1}$11] //α-Fe[$\bar{1}$11]. When $T_s = 100\,°C$ and 200 °C, the Fe–N films contain more α'-martensite and γ'-Fe_4N, respectively. The integrated electron diffraction pattern of the α''-$Fe_{16}N_2$ single crystal in the [$\bar{1}$11] direction was clearly observed. The film revealing a single-crystal electron diffraction pattern exhibits a high saturation magnetization M_s up to 2050 emu cc^{-1}, and this confirms the high M_s of the α''-$Fe_{16}N_2$ phase.

1. Introduction

In the early 1970s, Kim and Takahashi [1] observed a giant saturated magnetic flux density ($B_s = 2.58\,T$) which was 17% stronger than that of pure iron. Believing that the Fe–N film was a polycrystalline mixture of Fe and α''-$Fe_{16}N_2$, they deduced that the B_s of α''-$Fe_{16}N_2$ would be 2.83 T from the volume ratio of $Fe_{16}N_2$ in the film. Since the large saturated flux density is of importance, both theoretically and from the point of view of practical applications, many researchers have made great efforts using a variety of methods to synthesize $Fe_{16}N_2$ into bulk materials [2–4] and thin films [5–15]. However, most deposition techniques lead to multiphase films; only a few have succeeded in fabricating single-crystal α''-$Fe_{16}N_2$. It is likely that the α''-$Fe_{16}N_2$ phase with a body-centred tetragonal (BCT) structure (see figure 1) is metastable. This has been clarified by Jack in his systematic pioneer study of the Fe–N phase diagram [16].

By using nitrogen ion implantation, Nakajima and Okamoto [7–9] transformed an Fe epitaxial film on an MgO substrate into nitrogen martensite Fe_xN and its ordered form α''-$Fe_{16}N_2$. The amount of α''-$Fe_{16}N_2$ increased from 16 wt% to 26 wt% by annealing it in a vacuum at 150 °C for 2 h. Gao and co-workers [10] recently found the presence of polycrystalline α''-$Fe_{16}N_2$ in selected area electron diffraction (SAD) rings.

0953-8984/95/183667+08$19.50

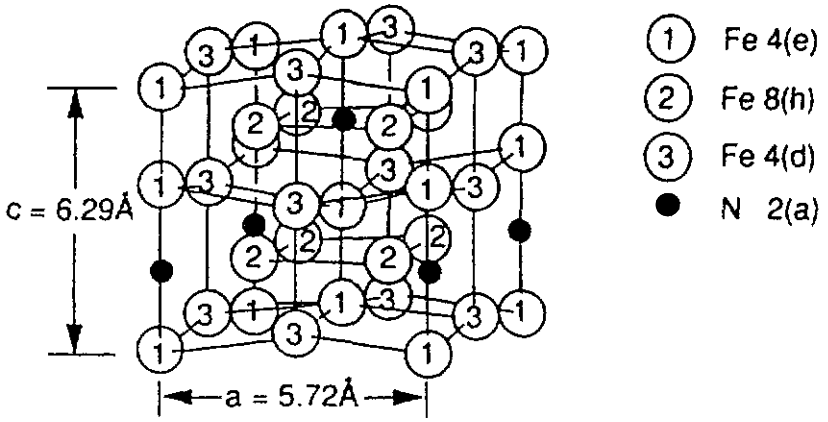

Figure 1. The crystal structure of α''-$Fe_{16}N_2$ [16].

Komuro and his co-workers [11, 12] have succeeded in growing single-crystal α''-$Fe_{16}N_2$ films by molecular beam epitaxy (MBE) in a nitrogen gas atmosphere on $Fe(100)/In_{0.2}Ga_{0.8}As(100)$ substrates. They reported that the B_s was 2.8 T at room temperature. In their series of papers the B_s for α''-$Fe_{16}N_2$ films was found to be 3.2 T at liquid-He temperatures, which corresponds to an average magnetic moment of 3.5 μ_B per Fe atom and is far beyond the Slater–Pauling curves. They also gave the first SAD pattern of α''-$Fe_{16}N_2$ single crystals by a transmission electron microscope (TEM), though the diffraction spots did not exhibit perfect symmetry in the spatial distribution.

Two problems remain to be solved in the study of α''-$Fe_{16}N_2$. First, the giant magnetic moment was only reconfirmed by MBE experiments and its origin is still mysterious. Second, the very low deposition rate of MBE limits its technological use. In our previous work we described epitaxial growth of Fe single-crystal films by facing targets sputtering (FTS) [17] and the preparation of Fe–N films containing the α''-$Fe_{16}N_2$ phase [18]. In order to obtain Fe–N films with a large amount of α''-$Fe_{16}N_2$ for use in high-density magnetic recording heads, we studied comprehensively the formation of various Fe–N phases depending on the different sputtering conditions. In this paper we report recent progress in our work on the production of α''-$Fe_{16}N_2$ single-crystal films and its distinctive integrated transmission electron microscope SAD patterns.

2. Experimental procedure

The Fe–N films were prepared by FTS onto NaCl (100) single crystals with a freshly cloven surface. The lattice constant of single-crystal NaCl is 5.63 Å which is only smaller by 1.6% than that of the a axis of $Fe_{16}N_2$ (5.72 Å), which provides the possibility of epitaxial growth. In an FTS system, the film can grow without the bombardment of high-energy particles, as in other sputtering deposition methods, and the deposition rate and substrate temperature can be easily controlled. The targets used here were a pair of iron (99.99%) discs 100 mm in diameter. The sputtering and reactive gases were Ar (99.999%) and N_2 (99.999%) respectively. The base pressure was 6×10^{-5} Pa. During sputtering, the partial pressures of the Ar and N_2 gases were held constant at 0.3 Pa and 0.05 Pa, respectively. Thin Fe films (100 Å) were deposited onto the substrates prior to the deposition of Fe–N

films. The deposition rate was about 2.0 Å s^{-1}. The effect of the substrate temperature (T_s) on the formation of the Fe–N phases was investigated in detail.

The crystal structure was examined with a Rigaku x-ray diffractometer (XRD) with CuKα radiation and a Hitachi H-9000 300 keV high-resolution transmission electron microscope (HRTEM). The saturation magnetization was measured with a vibrating sample magnetometer (VSM) in a magnetic field of 8 kOe at room temperature. The thickness of the film was measured by the multi-beam interference method.

3. Results and discussion

3.1. Substrate temperature dependence of formed phases in Fe–N films

To manifest the influence of the substrate temperature T_s on the formation of Fe–N phases and their morphology, Fe–N films were grown at different T_s with the other sputtering parameters kept identical. It was found from experiment that the phases were quite diversified at different T_s. To make these cases comparable, the film thickness was fixed at 400 Å.

It should be noted that the lattice parameters of α'-martensite varied with the nitrogen concentration. Under our conditions, the nitrogen concentration was 11.0 at.%, as obtained by x-ray photoelectron spectroscopy from the integrated intensity of Fe 2p and N 1s peaks with reference to Fe_4N pure powder. The lattice parameters were $a = b = 2.846$ Å and $c = 3.126$ Å, according to [16]. The M_s of α'-martensite is estimated to be ~ 1860 emu cc^{-1} [3].

Figure 2 shows the XRD patterns of Fe–N films deposited at different T_s. When $T_s = 100\,^{\circ}C$, the peaks of α-Fe (110) overlapping α''-$Fe_{16}N_2$ (220), α'-martensite (112) and (211) appear. When $T_s = 150\,^{\circ}C$, there appear only an intense peak of α''-$Fe_{16}N_2$ (220) (partially including an overlapped α-Fe (110)) and a weak peak of γ'-Fe_4N (221, 300). When $T_s = 200\,^{\circ}C$, we find peaks of ϵ-Fe_xN ($2 < x \leqslant 3$) ((100), (103)) in the pattern along with the peaks of α-Fe (110), α''-$Fe_{16}N_2$ ((112), (022), (220)) and γ'-Fe_4N ((211), (311)). Some information is completely covered in the intensive NaCl (002) and (004) peaks. Figure 3(*a*) shows the SAD pattern and TEM bright image of Fe–N films deposited at $T_s = 100\,^{\circ}C$. The indexing results are listed in table 1. One can see that there are γ'-Fe_4N, α-Fe, α''-$Fe_{16}N_2$ and α'-martensite picked out from the SAD pattern. Figure 3(*b*) shows the SAD pattern and TEM bright image of an Fe–N film deposited at $T_s = 150\,^{\circ}C$. There are polycrystalline rings of γ'-Fe_4N (110) and (221, 300), α-Fe (110) and α''-$Fe_{16}N_2$ (114), as indexed in table 2. Also, the diffraction spots of single-crystal α''-$Fe_{16}N_2$ are marked, as shown in figure 4. The spots are integrated and display a quasi-sixfold symmetry, which is denoted as a tetragonal body-centred lattice with $a = b = 5.72$ Å and $c = 6.29$ Å. This pattern is the stereographic projection in the $[\bar{1}11]$ direction of single-crystal α''-$Fe_{16}N_2$. It is also shown in its XRD pattern that α''-$Fe_{16}N_2$ has the same crystallographic orientation as α-Fe. From the point of view of x-ray diffractometry, it is regarded that α''-$Fe_{16}N_2$ grows epitaxially on the α-Fe (110) substrate. The following orientation relationship between α''-$Fe_{16}N_2$ and α-Fe is calculated:

$$\alpha'' - Fe_{16}N_2(110)//\alpha - Fe(110) \qquad \alpha'' - Fe_{16}N_2[\bar{1}11]//\alpha - Fe[\bar{1}11].$$

The interplanar spacing of α''-$Fe_{16}N_2$ (110) is 4.045 Å, while that of Fe (110) is 2.022 Å. The unit cell of α''-$Fe_{16}N_2$ grows on 2×2 unit cells of α-Fe. The mismatch between $Fe_{16}N_2$

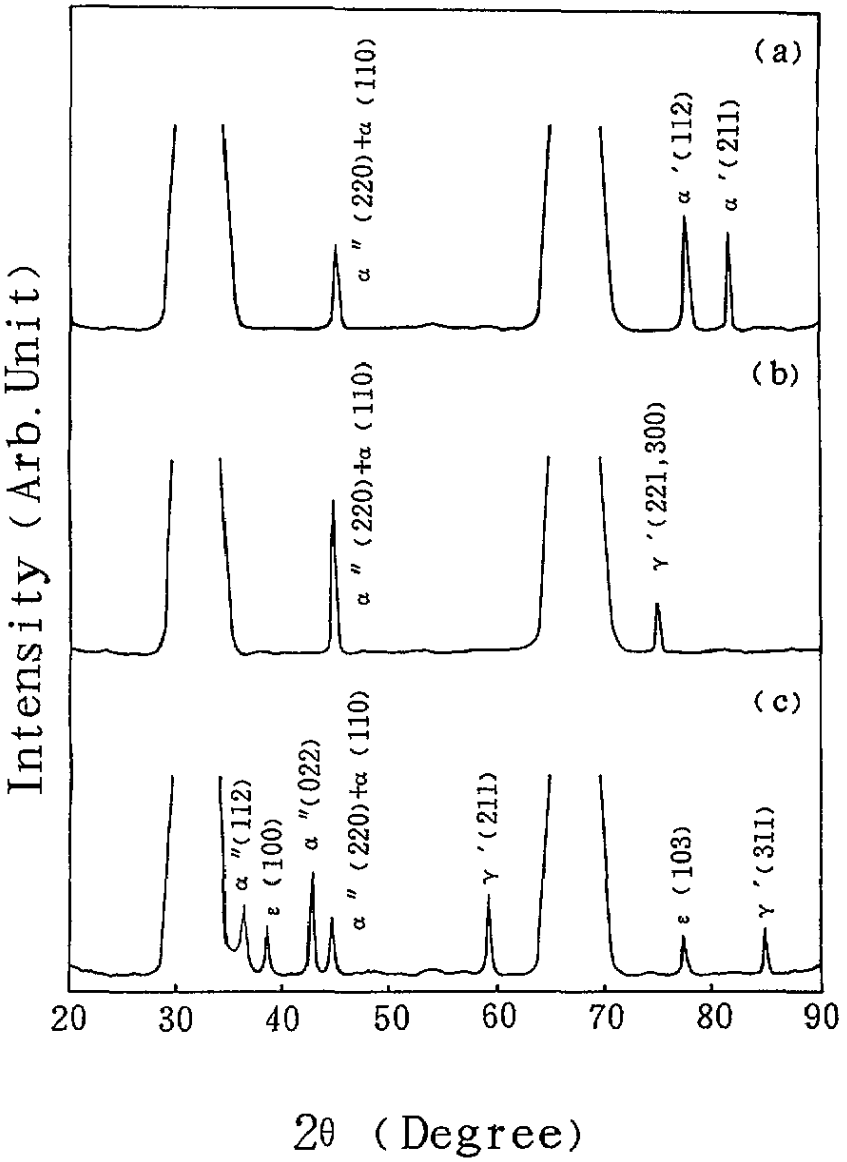

Figure 2. *X-ray diffraction patterns of Fe–N films deposited at (a) $T_s = 100\,^{\circ}C$, (b) $T_s = 150\,^{\circ}C$ and (c) $T_s = 200\,^{\circ}C$.*

and Fe is as small as 0.25%, and therefore epitaxial growth with this orientation relationship is advantageous.

By the Scherrer formula, the calculated mean crystalline size $\langle D \rangle$ of single-crystal α''-$Fe_{16}N_2$ is about $\sim 150\,\text{Å}$ from the full width at half maximum of the peak in the XRD pattern. This figure agrees well with the result from the TEM image. It should be noted that the selected area in SAD patterns is of the order of μm in diameter. Accordingly, it can be confirmed that the film consists of a number of highly oriented single-crystal grains of α''-$Fe_{16}N_2$, as shown in the TEM image in figure 3(*b*).

Table 1. Indexing results for the Fe–N film deposited at $T_s = 100\,°C$.

d_{exp} (Å)	Phase (*hkl*)	d_{calc} (Å)	Intensity
2.68	γ' (110)	2.68	Weak
2.50	α'' (112)	2.48	Weak
2.02	α (110)	2.03	Medium
1.71	γ' (210)	1.70	Medium
1.41	α' (200)	1.42	Strong
1.23	α' (112)	1.23	Strong
1.17	α' (211)	1.18	Strong

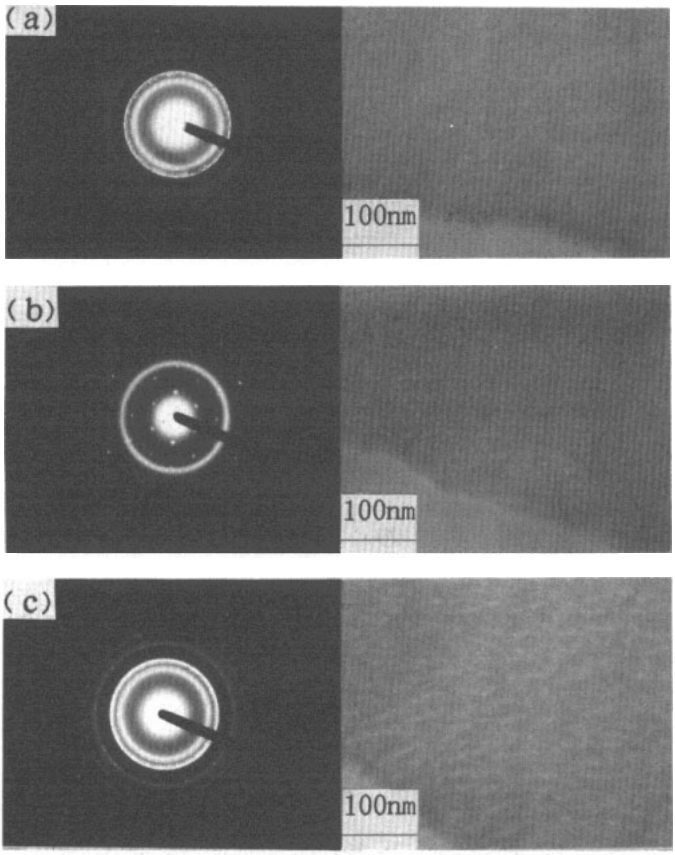

Figure 3. The selected area electron diffraction patterns and bright-field images of Fe–N films deposited at (*a*) $T_s = 100\,°C$, (*b*) $T_s = 150\,°C$, and (*c*) $T_s = 200\,°C$. The image in (*b*) corresponds to the patterns of single-crystal α''-$Fe_{16}N_2$ with $[\bar{1}11]$ incidence.

Figure 3(*c*) shows the SAD pattern and TEM bright image of the Fe–N film obtained at $T_s = 200\,°C$. The related indexing results are listed in table 3. There are α-Fe, α''-$Fe_{16}N_2$, γ'-Fe_4N and ϵ-Fe_xN ($2 < x \leqslant 3$) identified in the pattern. From the XRD pattern, we find that the first and second dominant phases are γ'-Fe_4N and α''-$Fe_{16}N_2$. The substrate temperature may influence the diffusion process of the atoms on the substrate, and at a higher T_s, the nitrogen atoms behave more actively. Therefore it is more likely to form more γ'-Fe_4N with a high nitrogen concentration.

Table 2. Indexing results for the Fe–N film deposited at $T_s = 150\,°C$ (except the patterns risen from $Fe_{16}N_2$ single crystal).

d_{exp} (Å)	Phase (*hkl*)	d_{calc} (Å)	Intensity
2.68	γ' (110)	2.68	Medium
2.03	α (110)	2.03	Medium
1.48	α'' (114)	1.47	Strong
1.25	γ' (221, 300)	1.27	Medium

Table 3. Indexing results for the Fe–N film deposited at $T_s = 200\,°C$.

d_{exp} (Å)	Phase (*hkl*)	d_{calc} (Å)	Intensity
2.49	α'' (112)	2.48	Medium
2.32	ϵ (100)	2.34	Medium
2.14	α'' (022)	2.12	Medium
2.04	α (110)	2.03	Strong
1.56	γ' (211)	1.55	Strong
1.36	γ' (220)	1.34	Strong
1.22	ϵ (103)	1.23	Medium
1.14	γ' (311)	1.14	Weak

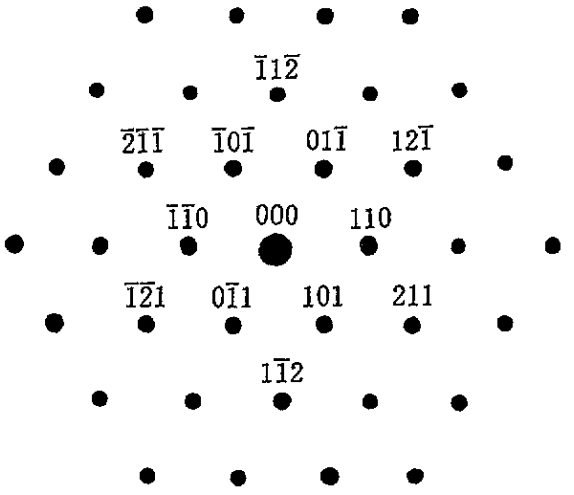

Figure 4. The illustration of the electron diffraction pattern corresponding to figure 3(*b*) of single-crystal α''-$Fe_{16}N_2$ with $[\bar{1}11]$ incidence.

Comparing the morphology of the three samples mentioned above, one can see that a higher substrate temperature leads to a larger grain size from the TEM images.

In summary, according to our experiments the substrate temperature plays a decisive role in Fe–N phase formation. When $T_s = 150\,°C$, it is advantageous to the growth of single-crystal α''-$Fe_{16}N_2$; at a lower T_s (100 °C), the phase is mainly α'-martensite with a stoichiometric concentration of $Fe_{16}N_2$; at a higher T_s (200 °C) more γ'-Fe_4N with a higher nitrogen concentration forms. In other words, the phase formation is very sensitive to the substrate temperature.

3.2. Saturation magnetization of Fe–N films

Table 4 shows the dependence of different phases and saturation magnetization of Fe–N films on T_s. The sample deposited at $T_s = 150\,°C$, in which $Fe_{16}N_2$ single crystals gathered, has $M_s = 2050\,\text{emu}\,\text{cc}^{-1}$, which is larger than that of pure iron by 21%. The volume ratio of $Fe_{16}N_2$ is estimated to be $\sim 70\%$ from the XRD pattern by subtracting the part of the Fe (110) thin film measured independently. And the M_s of $Fe_{16}N_2$ is expected to be $2200\,\text{emu}\,\text{cc}^{-1}$, which is in accordance with the results of Kim and co-workers [1] and Komuro and co-workers [11]. It is quite different from the theoretically calculated values by Sakuma [19], Min [20] and Coehoorn and co-workers [21]. Thus the origin of the giant magnetization is still confusing. According to Sugita and co-workers [12] and Nakajima and co-workers [9], the volume expansion and charge transfer effects are responsible for the high saturation magnetization of $Fe_{16}N_2$. In fact, the authors have observed considerable binding energy shifts of Fe and N atoms in $Fe_{16}N_2$ single crystals by x-ray photoelectron spectroscopy. The results observed will be published elsewhere. The recent inspiring theoretical work by Papanikolaou and co-workers [22] indicates that N, as both substitutional and interstitial impurities in alkali metals, may have quite a sizable magnetic moment of between 1.5–3.0 μ_B. According to these authors we should take into account the moment of N atoms in a more satisfactory manner, rather than accept the previous rather unsatisfactory theoretical results, such as 0.06 μ_B by Min [20] and $-0.03\,\mu_B$ by Coehoorn and co-workers [21]. We hope that this idea will prompt theoretical work on the origin of the strangely high saturation magnetization of $Fe_{16}N_2$.

Table 4. Phase and saturation magnetization dependence on T_s.

T_s(°C)	All phases	Dominant phase	M_s (emu cc^{-1})
100	$\alpha + \alpha' + \alpha''$	α'	1800
150	$\alpha + \alpha'' + \gamma'$	α''	2050
200	$\alpha + \gamma' + \epsilon + \alpha''$	$\alpha'' + \gamma'$	1600

The films deposited at $T_s = 100\,°C$ and 200 °C do not have the same saturation magnetization as at 150 °C. As well as the α and α'' phases, there are α' ($\sim 1860\,\text{emu}\,\text{cc}^{-1}$) and γ' ($\sim 1400\,\text{emu}\,\text{cc}^{-1}$) phases in the former case, and γ' and ϵ phases in the latter case. It is difficult to estimate quantitatively the volume ratio of these phases in the films from the XRD patterns because some peaks of the Fe–N phases are completely covered in the peaks of single-crystal NaCl (002) and (004), and other peaks overlap.

4. Conclusion

α''-$Fe_{16}N_2$ single-crystal films can be successfully prepared by the FTS method onto single-crystal NaCl (001) substrates, at a deposition rate as high as $2.0\,\text{Å}\,\text{s}^{-1}$. The formed phases are strongly dependent on the substrate temperature. At $T_s = 150\,°C$, single crystals of α''-$Fe_{16}N_2$ grow epitaxially on α-Fe with an orientation relationship of α''-$Fe_{16}N_2$ (110)//α-Fe (110) and α''-$Fe_{16}N_2$ [$\bar{1}$11]//α-Fe [$\bar{1}$11]. The integrated electron diffraction pattern of the α''-$Fe_{16}N_2$ single crystal in the [$\bar{1}$11] direction has been observed distinctly for the first time. The film revealing single-crystal electron diffraction patterns exhibits a high saturation magnetization M_s up to $2050\,\text{emu}\,\text{cc}^{-1}$, and this confirms the high M_s of the α''-$Fe_{16}N_2$ phase; the origin of this giant magnetization remains unclear.

Acknowledgments

This work is financially supported by the National Natural Science Foundation of China. The authors are grateful to the researchers in the TEM laboratory of Peking University and in the x-ray laboratory of Nankai University for their assistance.

References

[1] Kim T K and Takahashi M 1972 *Appl. Phys. Lett.* **20** 492
[2] Bao X H, Metzger R M and Corbuicchio M 1994 *J. Appl. Phys.* **75** 5870
[3] Huang M Q, Wallace W E, Simizu S, Pedziwiatr A T and Obermyer R T 1994 *J. Appl. Phys.* **75** 6574
[4] Coey J M D, Donnell K O, Qi Q N, Touchais E and Jack K H 1994 *J. Phys.: Condens. Matter* **6** L23
[5] Kano A, Kazama N S, Fujimori H and Takahashi T 1982 *J. Appl. Phys.* **53** 8332
[6] Morisako A, Takahashi K, Matsumoto M and Naoe M 1988 *J. Appl. Phys.* **63** 3230
[7] Nakajima K, Okamoto S and Okada T 1989 *J. Appl. Phys.* **65** 4357
[8] Nakajima K, Okamoto S 1990 *Appl. Phys. Lett.* **56** 92
[9] Nakajima K, Yamashita T, Takata M and Okamoto S 1991 *J. Appl. Phys.* **70** 6033
[10] Gao C, Doyle W D and Shamsuzzoha M 1993 *J. Appl. Phys.* **73** 6579
[11] Komuro M, Kozono Y, Hanozono M and Sugita Y 1990 *J. Appl. Phys.* **67** 5126
[12] Sugita Y, Mitsuoka K, Komuro M, Hoshiya H, Kozono Y and Hanozono M 1991 *J. Appl. Phys.* **70** 5977
[13] Takahashi M, Shoji H, Takahashi H and Wakiyama T 1993 *IEEE Trans. Magn.* **29** 3040
[14] Russak M A, Jahnes C V, Klokholn E, Lee J W, Re M E and Webb B C 1991 *J. Appl. Phys.* **70** 6427
[15] Kopcewicz M, Jagielski J, Turos A and Williamson D L 1992 *J. Appl. Phys.* **71** 4217
[16] Jack K H 1951 *Proc. R. Soc.* A **208** 216
[17] Jiang E Y, Zhang X X, Li J E and Liu Y G 1987 *IEEE Trans. Magn* **23** 2139
[18] Sun D C, Jiang E Y, Liu H, Liu M S and Lin C 1994 *J. Phys. D: Appl. Phys.* **27** (at press)
[19] Sakuma A 1991 *J. Magn. Magn. Mater.* **102** 127
[20] Min B I 1992 *Phys. Rev.* B **46** 8232
[21] Coehoorn R, Daalderop G H O and Jansen H J F 1993 *Phys. Rev.* B **48** 3830
[22] Papanikolaou N, Stefanou N, Zeller R, Dederichs P H 1993 *Phys. Rev. Lett.* **71** 629